Optics
2025, Vol. 13, No. 2, pp. 24-32
https://doi.org/10.11648/j.optics.20251302.12

Research Article

Versatile Protrusive VO_2 Metamaterials Enabling Tunable Ultra-broadband Terahertz Absorption

Yong-Rok Han[1], Kwang-Hyok Kim[1], Kwang-Jin Ri[2, *]

[1]Institute of Information Technology, University of Sciences, Pyongyang, Democratic People's Republic of Korea
[2]Department of Physics, University of Sciences, Pyongyang, Democratic People's Republic of Korea

Abstract

Until now, it has been conventional to design tunable metamaterial absorbers with single layer scheme of metal-dielectric-VO_2. For further expansion of the operating bandwidth, the construction method stacking several layers of dielctric-VO_2 has been utilized. However, the single layer configuration of metal-dielectric-VO_2 cannot extend the absorption bandwidth to the entire THz band. Meanwhile, In the stacking method, other VO_2 resonators excepting the topmost VO_2 resonator are embedded in the dielectric substrate. This unavoidably leads to the delay in response time to external stimuli. So, apart from these conventional methods, we have conceived the protrusive VO_2 metamaterials, which are effective for overcoming the above limitations. The protrusive VO_2 metamaterials consist of a VO_2 square ring, a protrusive VO_2 square patch and a polyimide substrate backed with a gold bottom plane. Based on the proposed design idea, we demonstrate a tunable ultra-broadband THz metamaterial absorber (MA) with bandwidth of 9.39 THz. That is, the protrusive VO_2 metamaterials greatly enlarge the operating bandwidth with perfect absorption. The proposed MA can obtain the absorptivity above 90% in range of 1.67-11.06 THz, with relative absorption bandwidth of 147.52%. Moreover, the protrusive VO_2 metamaterials can realize the absorption tunability by modifying the conductivity of VO_2. Additionally, we also demonstrate that the idea of protrusive VO_2 metamaterials is very useful for designing several tunable ultra-broadband THz MAs. Owing to the excellent structural versatility, the protrusive VO_2 metamaterials are of great value for THz applications.

Keywords

Metamaterial Absorber, Versatile, Protrusive, Tunable, Terahertz, Vanadium Dioxide

1. Introduction

Terahertz (THz) wave ranging from 0.1 THz to 10 THz is a relatively unexplored regime of the electromagnetic spectrum and is so called the THz gap, because there is a lack of efficient THz generators and detectors [1]. Luckily, the concept of metamaterials has provided great possibilities to pioneer the "THz gap". Metamaterials are artificially engineered materials with unique properties absent from natural materials, and have numerous applications ranging from switches [2], to antennas [3, 4], absorbers [5-8], and filters [9, 10]. Among those, THz MAs play critical roles in security imaging [11], biological sensing [12], explosive detecting [13] and so on. The THz MA [14] was firstly developed in 2008. Since then,

*Corresponding author: rkj1994@star-co.net.kp (Kwang-Jin Ri)

Received: 1 August 2025; **Accepted:** 15 August 2025; **Published:** 8 September 2025

numerous THz MAs including multiband [15-17] and broadband [18-20] absorbers have been studied based on the initial metal-dielectric-metal configuration. However, these THz MAs are not capable of adjusting the absorptivity after fabrication, which seriously blocks their potential applications in some practical areas such as modulators, sensors and switches. As the cure for this problem, researchers have developed tunable MAs whose absorptivities are changed by controlling the external stimuli including heat, electric field and light [21-23].

Particularly, tunable THz MAs based on VO_2 have drawn lots of attentions due to their good performances such as broadband absorption, great modulation depth and fast response property [24-26]. Since VO_2 is a phase transition material, it has different conductivities when the environmental temperature is varied, and the change of conductivity of VO_2 directly influences its relative permittivity. Consequently, VO_2-based MAs have the absorption tunability depending on the environmental temperature.

Similar to conventional THz MAs with metal-dielectric-metal configuration, it is very necessary for practical applications to extend the operating bandwidth of tunable THz MAs by using the relatively simple structures [27-31]. For this reason, many tireless efforts have been dedicated to designing tunable broadband THz MAs with simple structures until now. For example, Gevorgyan et al [32] demonstrated a tunable ultra-broadband THz MA based on simple VO_2 strips, whose absorptivity is higher than 90% in the operating range of 0.66-1.84 THz. Ahmed et al [33] investigated an auxetic ultra-broadband THz MA with two M-shaped VO_2 rings, whose absorptivity can reach above 90% between 4.15 THz to 8.43 THz. Yang et al [34] proposed a tunable ultra-broadband THz MA with a single square VO_2 patch, which can obtain absorptivity more than 90% in the operating range of 1.07-4.92 THz. Wang et al [35] also investigated a tunable broadband THz MA with a VO_2 patterned resonator, which can work from 2.82 THz to 9.17 THz with absorptivity above 90%. Zhu et al [36] conceived a tunable broadband THz MA based on circular VO_2 pattern, whose absorptivity is higher than 90% in the operating range of 2.32-7.51 THz. Besides, several studies on tunable ultra-broadband THz MAs with simple structures have been reported [37-41]. Despite these endeavors, further extending the operating bandwidth of tunable MAs with simple structures still remains a challenge.

Until now, it has been conventional to design tunable MAs with single layer scheme of metal-dielectric-VO_2. For further expansion of the operating bandwidth, the construction method stacking several layers of dielctric-VO_2 has been utilized. However, the single layer configuration of metal-dielectric-VO_2 cannot extend the absorption bandwidth to the entire THz band. Meanwhile, In the stacking method, other VO_2 resonators excepting the topmost VO_2 resonator are embedded in the dielectric substrate [39-41]. This unavoidably leads to the delay in response time to external stimuli.

So, apart from these conventional methods, we have conceived the protrusive VO_2 metamaterials, which are effective for overcoming the above limitations. Unlike previous studies which only reported tunable broadband THz MAs themselves, we focus on the versatile scheme of protrusive VO_2 metamaterials enabling tunable ultra-broadband absorption. Simulation results demonstrate that all the four kinds of MAs using the slightly modified protrusive VO_2 metamaterials can successfully achieve tunable ultra-broadband absorption at THz regime. Compared with previous tunable THz MAs [24-41], the protrusive VO_2 metamaterials significantly expands the bandwidth retaining absorptivity above 90% and can obtain the excellent absorption tunability. The principle of ultra-broadband absorption of protrusive VO_2 metamaterials is elucidated by means of electric and magnetic field distributions. The effects of geometrical dimensions on the absorption characteristics are investigated. Owing to the excellent features such as ultra-broadband absorption, simple structure and absorption tunability, our designed protrusive VO_2 metamaterials are of great value for applications such as modulating, imaging, detecting, switching et al.

2. Design and Simulation

Figure 1 shows the geometry of proposed MA composed of protrusive VO_2 metasurface, polyimide substrate and gold bottom plane. The proposed MA has the periodicity of $P = 27\,\mu\text{m}$, while the metasurface side lengths are $L_1 = 21.5\,\mu\text{m}$ and $L_2 = 12.5\,\mu\text{m}$, respectively. The thickness of gold plane is $h_1 = 0.4\,\mu\text{m}$, while its conductivity is $\sigma = 4.561 \times 10^7$ S/m. The thicknesses of lower and upper polyimide substrates are $h_2 = 11\mu\text{m}$ and $h_4 = 9.5\mu\text{m}$, respectively. The relative permittivity of polyimide substrates is $\varepsilon = 3.5(1 + i0.0027)$. The thickness of VO_2 metasurface is $h_3 = 0.2\mu\text{m}$, while its relative permittivity is calculated by Drude model [42], that is:

$$\varepsilon(\omega) = \varepsilon_\infty - \frac{\omega_p^2(\sigma)}{(\omega^2 - i\gamma\omega)} \tag{1}$$

where, $\varepsilon_\infty = 12$ indicates the permittivity at infinite frequency, $\gamma = 5.75 \times 10^{13}$ rad/s represents the collision frequency. The plasma frequency is described as:

$$\omega_p^2(\sigma) = \frac{\sigma_{VO_2}}{\sigma_0}\omega_p^2(\sigma_0) \tag{2}$$

with $\sigma_0 = 3 \times 10^5$ S/m and $\omega_p(\sigma_0) = 1.4 \times 10^{15}$ rad/s. The conductivity values of VO_2 are 2×10^5 S/m and 200 S/m at $T = 350$ K and $T = 300$ K, respectively [43].

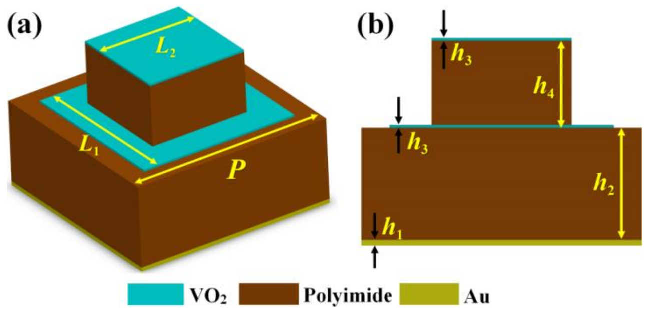

***Figure 1**. Unit cell of the proposed MA: (a) perspective view, (b) side view.*

We simulate the scattering parameters of MAs with the well-known software CST Studio Suite 2018. In the boundary condition setting, the unit cell condition is allocated to the x-direction and the y- direction. The open (add space) condition is allocated to the z-direction. In the simulation, the incident THz waves are sorted into two modes. One mode is a transverse electric (TE) wave in which electric field points the y-axis, and another mode is a transverse magnetic (TM) wave in which electric field points the x-axis [44]. The absorptivity of a MA is defined as $A(\omega) = 1 - |S_{11}(\omega)|^2 - |S_{21}(\omega)|^2$, where $|S_{11}(\omega)|^2$ and $|S_{21}(\omega)|^2$ indicate the reflectance and transmittance, respectively. For the conventional MAs, the gold bottom plane blocks the transmission, so $|S_{21}(\omega)|^2$ becomes zero. This simplifies the calculation of absorptivity as $A(\omega) = 1 - |S_{11}(\omega)|^2$.

3. Results and Discussion

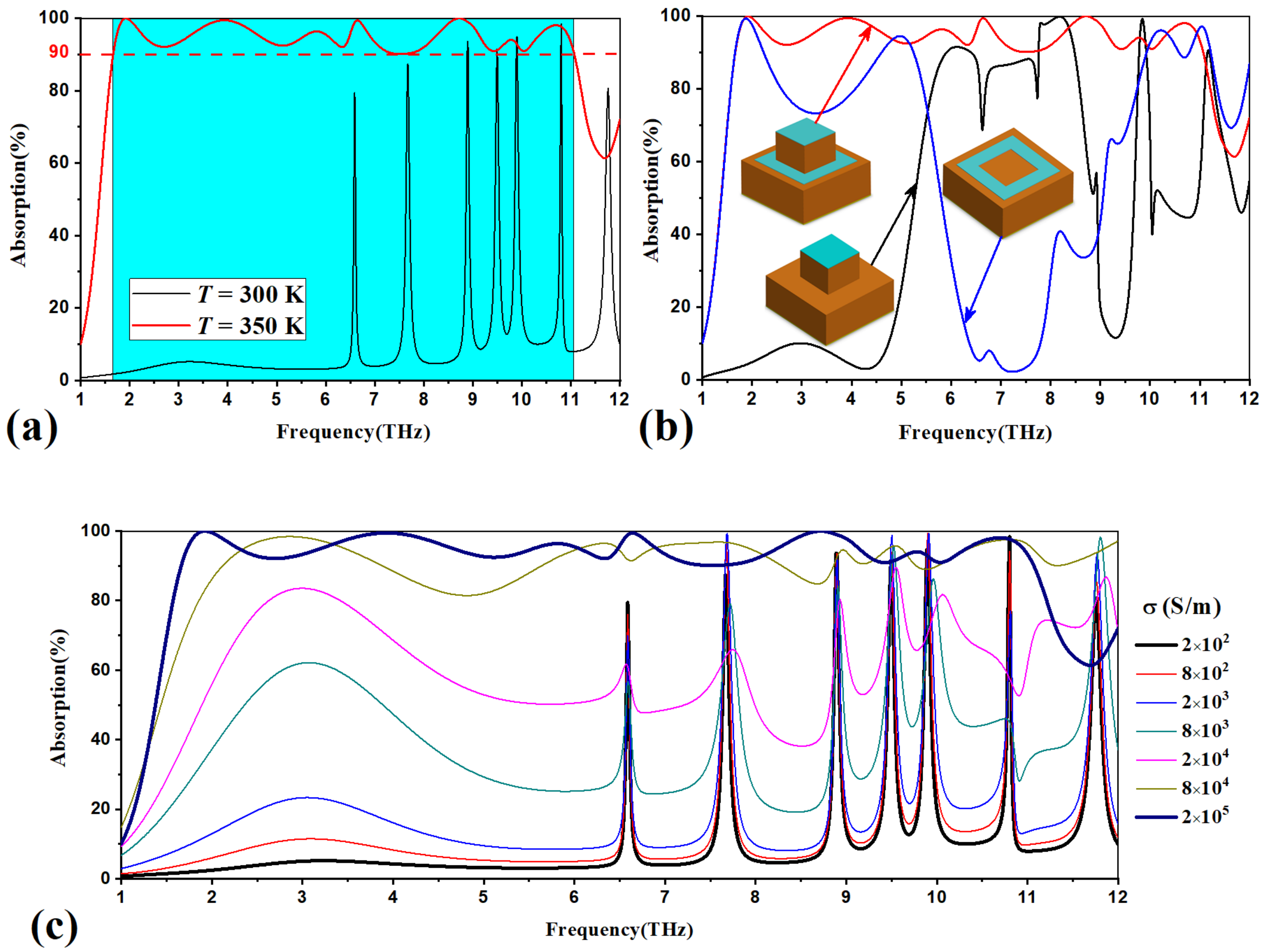

***Figure 2**. (a) Absorption spectra of proposed MA at different temperatures for TE wave, (b) Absorption spectra of three MAs with different resonant structures for TE wave, (c) Absorption spectra of proposed MA for different VO2 conductivities.*

The simulated absorption curves of designed MA for TE mode are displayed in Figure 2(a). The absorption efficiency of proposed MA is above 90% in the operating range of 1.67-11.06 THz, while its absorption bandwidth reaches 9.39 THz at $T = 350$ K. When $T = 300$ K, the above absorption property vanishes and the proposed MA acts as a reflector in the low frequency band, while there exist several resonant peaks in high frequency band. To reveal the influence of protrusive VO_2 metasurface structure on absorption performance, we simulate absorption spectra of three MAs with different resonant structures. As shown in Figure 2(b), the first MA with VO_2 square ring operates in the low frequency band, but the absorptivity in range of 2.23-4.61 THz is below 90%. The second MA with protrusive VO_2 square patch operates in the high frequency band, but the absorptivity fluctuates seriously. The combination of VO_2 square ring and protrusive VO_2 square patch results in the ultra-broadband absorption with bandwidth of 9.39 THz. The cause of opposite absorption behaviors at $T = 300$ K and $T = 350$ K lies in the phase transition property of VO_2. At $T = 300$ K, VO_2 works as an insulator (the conductivity $\sigma = 200$ S/m) and it behaves as a conductor (the conductivity $\sigma = 2 \times 10^5$ S/m) at $T = 350$ K. So, the detailed investigation of absorption tunability of the designed MA for different VO_2 conductivities is also desirable. As shown in Figure 2(c), one can adjust the absorptivity of designed MA by increasing the VO_2 conductivity from 200 S/m to 2×10^5 S/m. The modulation depth (MD) of tunable THz MAs becomes a vital factor for their practical applications, which is expressed as $MD = (A_m - A_i)/A_m \times 100$, where A_m and A_i indicate the absorptances for the metallic state and insulator state of VO_2, respectively [34]. As a result, our designed THz device achieves the modulation depth exceeding 90% in range of 1.6-6.5 THz. It means that the proposed THz device can act as an excellent ultra-broadband THz modulator. In practical applications of tunable THz MAs based on VO_2, the recommended adjusting method of VO_2 conductivity may be the photo-excited transition technique using strong laser pulses with the timescale below several picoseconds [45-47].

Table 1. *Comparison of the proposed MA prior MAs.*

Ref.	Absorption bandwidth (THz)	RAB (%)	Tunable range (%)	Thickness (μm)
[24]	3.83(3.25-7.08)	74.15	-	70.14
[25]	0.33(0.385-0.715)	60	30-100	70.5
[26]	2.3(6.6-8.9)	29.67	-	22.39
[27]	3(2.54-5.54)	74.25	10-100	10.6
[28]	4.5(3.5-8)	78.26	18-100	10.1
[29]	1(0.7-1.7)	83	3-90	31.4
[30]	1.56(2.07-3.63)	54.73	-	26.2
[31]	3.78(3.01-6.79)	77.14	2.7-98.9	8.2
[32]	1.18(0.66-1.84)	94.4	3-95	39.2
[33]	4.28(4.15-8.43)	68.04	2-100	8.9
[34]	3.85(1.07-4.92)	128.54	20-90	27.4
[35]	6.35(2.82-9.17)	105.92	2-100	8.38
[36]	5.19(2.32-7.51)	106.12	1.5-99.8	11.2
[37]	7.4(4.50-11.90)	90.18	2-98	6.25
This paper	9.39(1.67-11.06)	147.52	2.2-99.9	21.1

We estimated the performance of proposed MA by introducing the relative absorption bandwidth (RAB) calculated as Eq. 3, in which f_L and f_U indicate the lower and the upper frequencies of operating band where the absorptivity is above 90%. Despite the simple metasurface structure, the RAB of proposed MA is 147.52%, which is a significantly expanded operating bandwidth compared with prior broadband MAs listed in Table 1.

$$RAB = 2 \times \frac{f_U - f_L}{f_U + f_L} \quad (3)$$

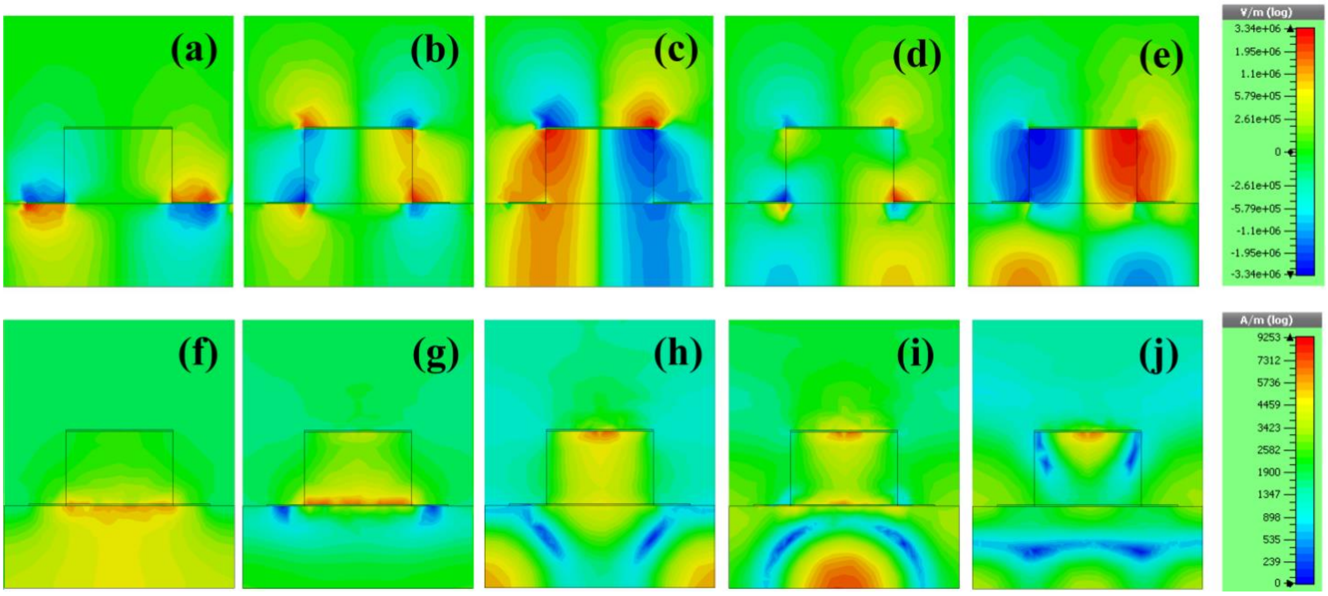

Figure 3. *Electric field (E_z) distributions (a-e) and Magnetic field ($|H_y|$) distributions (f-j) in the XOZ plane: (a, f) at 1.92 THz, (b, g) at 3.92 THz, (c, h) at 6.64 THz, (d, i) at 8.72 THz, (e, j) at 10.69 THz.*

To elucidate the ultra-broadband absorption principle, the distributions of electric (E_z) and magnetic fields ($|H_y|$) for several resonant peaks are investigated in detail. At f_1=1.92 THz, the electric field intensity is strengthened in the polyimide substrate around the VO_2 square ring as shown in Figure 3(a), resulting in the magnetic resonance in lower polyimide substrate as shown in Figure 3(f). At f_2=3.92 THz, the electric field is localized in the upper polyimide substrate between top VO_2 square patch and VO_2 square ring as shown in Figure 3(b). By this electric field distribution, the magnetic resonance in upper polyimide substrate is induced as shown in Figure 3(g). At f_3=6.64 THz, the electric field intensity is strengthened inside the upper and lower polyimide substrates as shown in Figure 3(c). As a result, the magnetic resonances are generated in both upper and lower polyimide substrates as shown in Figure 3(h). Here, the magnetic resonance in lower polyimide substrate is due to the coupling effect between neighboring unit cells. At f_4=8.72 THz, the electric field intensity is strengthened around the edge of top VO_2 square patch, inside the VO_2 square ring, and inside the lower polyimide substrate as shown in Figure 3(d), and then the magnetic resonances are excited as shown in Figure 3(i). Lastly, at f_5=10.69 THz, the electric field intensity is strengthened in both upper and lower polyimide substrates as shown in Figure 3(e). So, the magnetic resonances are induced as shown in Figure 3(j). To sum up, the ultra-broadband absorption of designed MA results from the overlap of five resonant frequencies which are based on the different magnetic resonances.

The simulated absorption spectra of designed MA with different geometrical parameters are given in Figure 4. As shown in Figure 4(a), the operating bandwidth of proposed MA decreases with the rise of periodic length P. This phenomenon is attributed to the resonance coupling effect between adjacent unit cells. As displayed in Figure 4(b), the lowest resonant frequency of proposed MA shows a redshift with the rise of side length L_1. As mentioned above, the VO_2 square ring directly affects the absorption at low frequency band. According to LC circuit model, the resonant frequency of proposed MA is reciprocally proportional to the resonator length. So, with the rise of L_1, the lowest resonant frequency undergoes redshift. Figure 4(c) demonstrates that the proposed MA has the broadest operating band in which the absorptivity exceeds 90% for $L_2 = 12.5\mu m$. As displayed in Figure 4(d), when the lower substrate thickness (h_2) is increased, the absorptivity at low frequency band remains steady, but the absorptivity at high frequency band arbitrarily changes. Because, thickness h_2 affects not only the interaction between gold ground plane and VO_2 square ring but also the interaction between gold ground plane and VO_2 square patch. Figure 4(e) exhibits the absorption responses for several values of the VO_2 thickness h_3. The proposed MA has the broadest operating band retaining over 90% absorptivity for $h_3 = 0.2\mu m$. This is because a good impedance matching condition between the designed MA and the free space is realized at $h_3 = 0.2\mu m$. Figure 4(f) shows the effect of upper substrate thickness on absorption performance. When the thickness h_4 is changed, the absorptivity of proposed MA remains nearly unchanged at low frequency band but undergoes a redshift at high frequency band. Because, the thickness h_4 directly affects the protrusive VO_2 square patch that is responsible for the absorption at high frequency band.

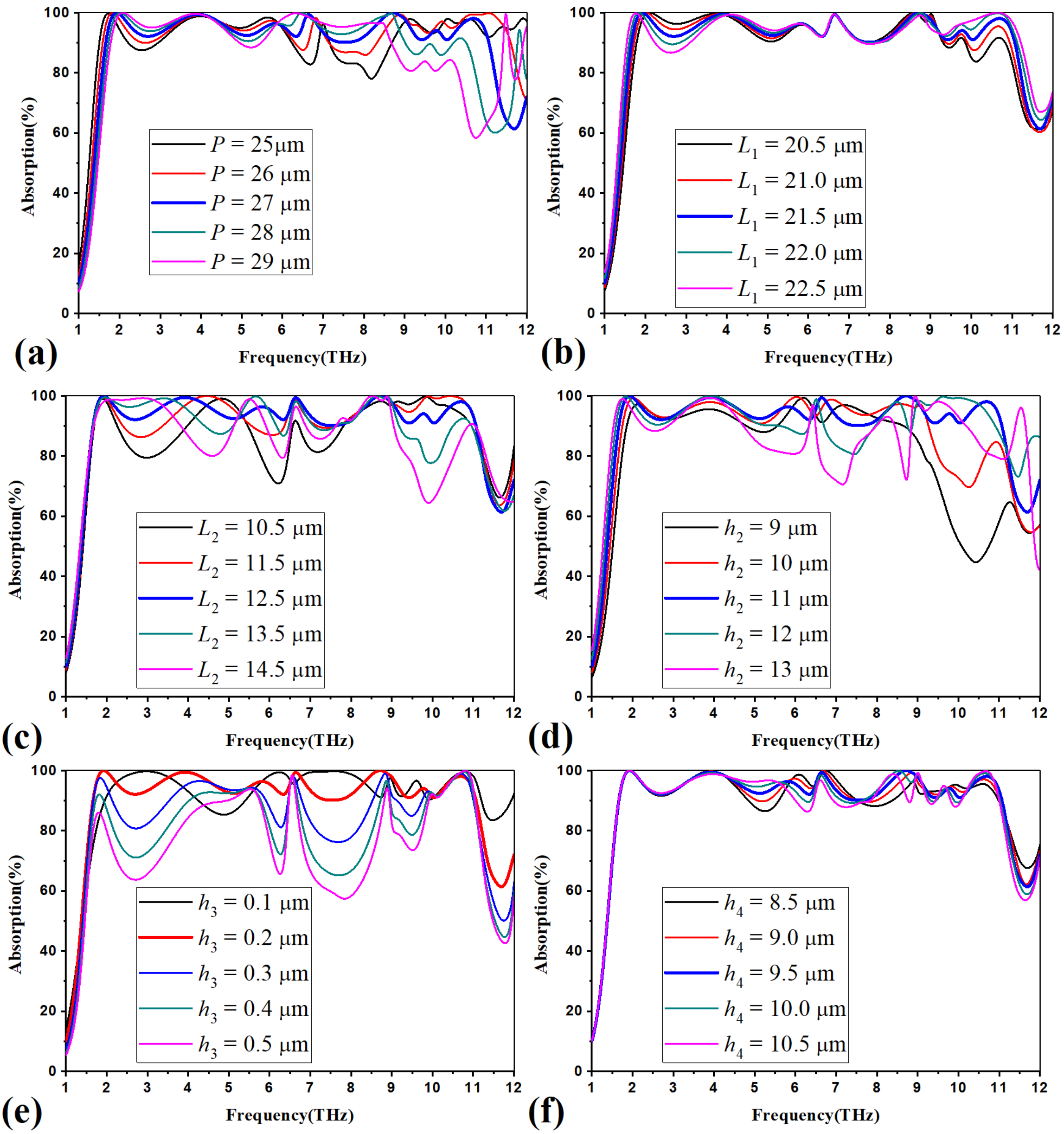

Figure 4. Absorption responses of proposed MA with change of geometrical dimensions: (a) P, (b) L_1, (c) L_2, (d) h_2, (e) h_3 and (f) h_4 for TE wave when T = 350 K.

We can easily obtain other tunable ultra-broadband THz MAs from the above-mentioned design idea. As shown in Figure 5, the unit cells of other MAs are constructed by combining the VO_2 circular ring, VO_2 circular patch, VO_2 square ring and VO_2 square patch. The optimized dimensions of the designed MAs are as follows: (a) $P = 26$μm, $D_1 =$ 23 μm, $D_2 = 14$ μm, $h_1 = 0.4$ μm, $h_2 = 10.8$ μm, $h_3 =$ 0.2 μm, $h_4 = 9$ μm, (b) $P = 27.3$ μm, $L = 21.5$ μm, $D =$ 14 μm, $h_1 = 0.4$ μm, $h_2 = 10.6$ μm, $h_3 = 0.2$ μm, $h_4 =$ 9.5 μm, (c) $P = 26$ μm, $L = 12$ μm, $D = 23.8$ μm, $h_1 =$ 0.4μm, $h_2 = 10.5$μm, $h_3 = 0.2$μm, $h_4 = 9$μm.

Figures 5(d)-5(f) shows the absorption responses of the MAs with different metasurface structures for TE wave. When $T = 350$ K, all the MAs exhibit ultra-broadband absorption performances. As shown in Figure 5(d), The first MA with VO_2 circular ring and protrusive VO_2 circular patch exhibits over 90% absorptivity in the operating range of 1.77-9.16 THz and its bandwidth is 7.39 THz. As shown in

Figure 5(e), the second MA with VO_2 square ring and protrusive VO_2 circular patch exhibits over 90% absorptivity in the operating range of 1.72-9.96 THz and the bandwidth reaches 8.24 THz. Figure 5(f) shows that the third MA with VO_2 circular ring and protrusive VO_2 square patch exhibits over 90% absorptivity in the operating range of 1.69-11.63 THz and the bandwidth reaches 9.94 THz. When $T = 300$ K, all the MAs act as a reflector in low frequency band, but have several resonant peaks in high frequency band.

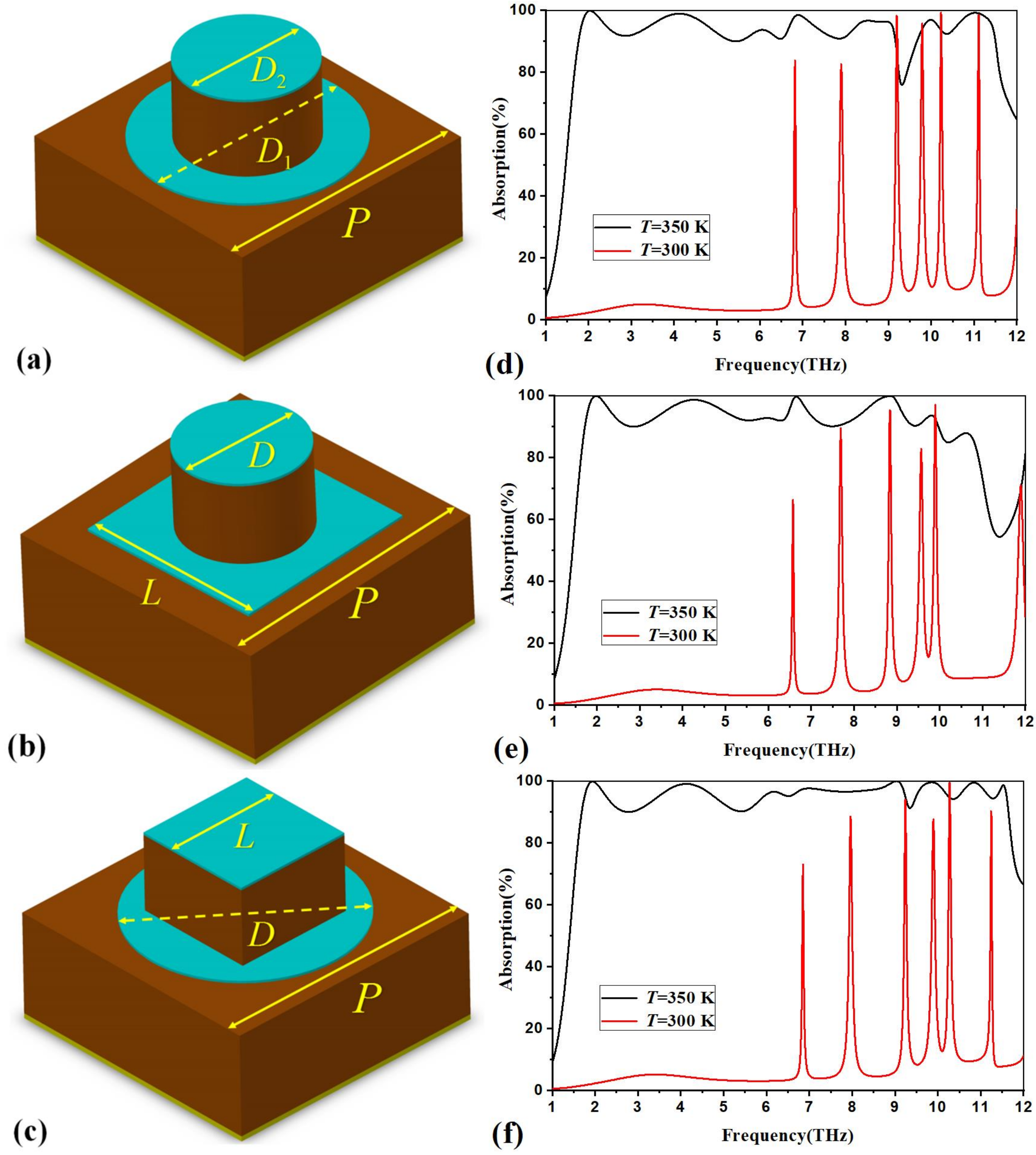

Figure 5. *Unit cells of several MAs with (a) VO_2 circular ring and protrusive VO_2 circular patch, (b) VO_2 square ring and protrusive VO_2 circular patch, (c) VO_2 circular ring and protrusive VO_2 square patch, (d) Absorption responses of the MA with VO_2 circular ring and protrusive VO_2 circular patch, (e) Absorption responses of the MA with VO_2 square ring and protrusive VO_2 circular patch, (f) Absorption responses of the MA with VO_2 circular ring and protrusive VO_2 square patch.*

4. Conclusion

A versatile scheme of protrusive VO_2 metamaterials enabling tunable ultra-broadband THz absorption has been investigated. To greatly expand the operating bandwidth and avoid the delay in response time, we conceived the versatile protrusive metasurface that combines the VO_2 square ring and protrusive VO_2 square patch. The absorptivity of designed MA is over 90% in the operating range of 1.67-11.06 THz at $T = 350$ K and such an operating bandwidth diminishes at $T = 300$ K. The RAB of proposed MA is 147.52%, which is greatly increased compared with other MAs [24-37]. Simulated electric field and magnetic field distributions show that magnetic resonances contribute to the ultra-broadband absorption. Moreover, our design idea is of great value for achieving several tunable ultra-broadband THz MAs. So, the protrusive VO_2 metamaterials may be very useful for THz imaging, biological sensing, material detecting, stealth technology and et al.

Abbreviations

MA	Metamaterial Absorber
THz	Terahertz
RAB	Relative Absorption Bandwidth
MD	Modulation Depth
TE	Transverse Electric
TM	Transverse Magnetic

Author Contributions

Kwang-Jin Ri: Conceptualization, Investigation, Writing – original draft
Yong-Rok Han: Investigation, Methodology
Kwang-Hyok Kim: Validation, Visualization

Conflicts of Interest

The authors declare no competing interests.

References

[1] U Nissanov and G Singh *Antenna Technology for Terahertz Wireless Communication* (Gewerbestrasse: Springer) (2023). https://doi.org/10.1007/978-3-031-35900-2

[2] L Guo, X Ma, Z Chang, C Xu, J Liao and R Zhang *J. Mater. Res. Technol.* 14 772 (2021). https://doi.org/10.1016/j.jmrt.2021.06.080

[3] C Caloz, T Itoh and A Rennings *IEEE Antennas Propag. Mag.* 50 25 (2008). https://doi.org/10.1109/MAP.2008.4674709

[4] L Si, K Han, R Niu, L Dong, W Xing and W Zhu *Opt. Express* 32 19352 (2024). https://doi.org/10.1364/OE.525260

[5] N I Landy, S Sajuyigbe, J J Mock, D R Smith and W J Padilla *Phys. Rev. Lett.* 100 207402 (2008). https://doi.org/10.1103/PhysRevLett.100.207402

[6] P T Bowen, A Baron and D R Smith *Phys. Rev. A* 93 063849 (2016). https://doi.org/10.1103/PhysRevA.063849

[7] X Yang, C Wang, M Qiao and X Li *J. Appl. Phys.* 137 133104 (2025). https://doi.org/10.1063/5.0260825

[8] S Sayed, K R Mahmoud and R I Mubarak *Sci. Rep.* 13 11937 (2023). https://doi.org/10.1038/s41598-023-38263-x

[9] S Badri and S Farkoush *Appl. Opt.* 60 2803 (2021). https://doi.org/10.1364/AO.60.002803

[10] N Niharika, S Singh and P. Kumar *Optik* 253 168551 (2022). https://doi.org/10.1016/j.ijleo.2021.168551

[11] R She, W Liu, Y Lu, Z Zhou and G. Li *Appl. Phys. Lett.* 115 021101 (2019). https://doi.org/10.1063/1.5094728

[12] H Zhou, C Yang, D Hu, D Li, X Hui, F Zhang, M Chen and X. Mu *Appl. Phys. Lett.* 115 143507 (2019). https://doi.org/10.1063/1.5111584

[13] H Zhu, K Wang, G Liu, J Mou, Y Wu, Z Zhang, Y Qiu and G Wei *Opt. Express* 30 15939 (2022). https://doi.org/10.1364/OE.456996

[14] H Tao, N I Landy, C M Bingham, X Zhang, R D Averitt and W J Padilla *Opt. Express* 16 7181 (2008). https://doi.org/10.1364/OE.16.007181

[15] A Faruk and C Sabah *Optik* 192 162976 (2019). https://doi.org/10.1016/j.ijleo.2019.162976

[16] B X Wang, C Tang, Q S Niu, Y H He and T Chen *Nanoscale Res. Lett.* 14 64 (2019). https://doi.org/10.1186/s11671-019-2876-3

[17] S Asgari and T Fabritius *IEEE Access* 10 63658 (2022). https://doi.org/10.1109/ACCESS.2022.3183272

[18] S J Guo, C X Hu and H F Zhang *J. Opt. Soc. Am. B* 37 2678 (2020). https://doi.org/10.1364/JOSAB.399048

[19] L Liu, W W Liu and Z Y Song *J. Appl. Phys.* 128 093104 (2020). https://doi.org/10.1063/5.0019902

[20] M W Jiang, Z Y Song and Q H Liu *Opt. Commun.* 471 125835 (2020). https://doi.org/10.1016/j.optcom.2020.125835

[21] R N Dao, X R Kong, H F Zhang and X R Su *Optik* 180 619 (2019). https://doi.org/10.1016/j.ijleo.2018.12.004

[22] L Zheng, R Feng, H Shi and X Li *Micromachines* 14 1715 (2023). https://doi.org/10.3390/mi14091715

[23] J N Zhang, G C Wang, B Zhang, T He, Y He and J L Shen *Opt. Mater.* 54 32 (2016). http://dx.doi.org/10.1016/j.optmat.2016.02.011

[24] M Zhang and Z Y Song *Opt. Express* 29 21551 (2021). https://doi.org/10.1364/OE.432967

[25] Z Y Song, K Wang, J W Li and Q H Liu *Opt. Express* 26 7148 (2018). https://doi.org/10.1364/OE.26.007148

[26] Y B Zhang, P H Wu, Z G Zhou, X F Chen, Z Yi, J Y Zhu, T S Zhang and H G Jile *IEEE Access* 8 85154 (2020). https://doi.org/10.1109/ACCESS.2020.2992700

[27] C Gandhi, P R Babu and K Senthilnathan *Front. Optoelectron.* 14 288 (2021). https://doi.org/10.1007/s12200-021-1223-3

[28] L S Wang, D Y Xia, Q H Fu, X Y Ding and Y Wang *Front. Mater.* 8 729495 (2021). https://doi.org/10.3389/fmats.2021.729495

[29] Y C Liu, Y X Qian, F R Hu, M Z Jiang and L H Zhang *Results Phys.* 19 103384 (2020). https://doi.org/10.1016/j.rinp.2020.103384

[30] Y S Zhou, H Xia, L M Zhang, Y F Zhao and W K Xie *Results Phys.* 22 103915 (2021). https://doi.org/10.1016/j.rinp.2021.103915

[31] G S Yang, F P Yan, X M Du, T Li, W Wang, Y L Lv, H Zhou and Y F Hou *AIP Adv.* 12 045219 (2022). https://doi.org/10.1063/5.0082295

[32] L Gevorgyan, H Haroyan, H Parsamyan and K Nerkararyan *RSC Adv.* 13 11948 (2023). https://doi.org/10.1039/d3ra01194a

[33] M R Ahmed, O Jyoti, F Farjana, P P Sarkar, A K Paul and M S Habib *Opt. Continuum* 3 2139 (2024). https://doi.org/10.1364/OPTCON.539561

[34] M J Yang, U S Jo, M C Ryu, Y G Pak and K J Ri *Indian J. Phys.* 99 673 (2025). https://doi.org/10.1007/s12648-024-03292-3

[35] Y J Wang, Y Y Chen, F Liu, L Chen, K Ji, X C Wang and X L Ji *Sci. Rep.* 15 10140 (2025). https://doi.org/10.1038/s41598-025-94645-3

[36] Y Zhu *Mater. Res. Express* 12 015801 (2025). https://doi.org/10.1088/2053-1591/ada41b

[37] M A Islam, M R Ahmed, O Jyoti, P P Sarkar and M S Habib *Opt. Continuum* 4 756 (2025). https://doi.org/10.1364/OPTCON.557405

[38] X F Jiao, Z H Zhang, T Li, Y Xu and G F Song *Appl. Sci.* 10 7259 (2020). https://doi.org/10.3390/app10207259

[39] H L Feng, Z X Zhang, J Y Zhang, D C Fang, J C Wang, et al. *Nanomaterials* 12 1731 (2022). https://doi.org/10.3390/nano12101731

[40] K J Ri and C H Ri *Opt. Commun.* 536 129377 (2023). https://doi.org/10.1016/j.optcom.2023.129377

[41] K J Ri, J S Kim, J H Kim and C H Ri *Opt. Commun.* 542 129573 (2023). https://doi.org/10.1016/j.optcom.2023.129573

[42] S Wang, L Kang and D H Werner *Sci. Rep.* 7 4326 (2017). https://doi.org/10.1038/s41598-017-0469

[43] Y Zhao, Q P Huang, H L Cai, X X Lin and Y L Lua *Opt. Commun.* 426 443 (2018). https://doi.org/10.1016/j.optcom.2018.05.085

[44] X R Kong, H F Zhang, R N Dao and G B Liu *J. Electron. Mater.* 48 4166-4169 (2019). https://doi.org/10.1007/s11664-019-07194-7

[45] A Cavalleri, C Tóth, C W Siders, et al. *Phys. Rev. Lett.* 87 237401 (2001). https://doi.org/10.1103/PhysRevLett.87.237401

[46] D J Hilton, R P Prasankumar, S Fourmaux, et al. *Phys. Rev. Lett.* 99 226401 (2007). https://doi.org/10.1103/PhysRevLett.99.226401

[47] Y Xiao, Z H Zhai, Q W Shi, et al. *Appl. Phys. Lett.* 107 031906 (2015). https://doi.org/10.1063/1.4927383